JOURNAL OF GEOPHYSICAL RESEARCH, VOL. 103, NO. C2, PAGES 3111-3118, FEBRUARY 15, 1998

Observations of swash under highly dissipative conditions

B. G. Ruessink, M. G. Kleinhans, and P. G. L. van den Beukel

Institute for Marine and Atmospheric Research Utrecht, Department of Physical Geography, Utrecht University, Utrecht, Netherlands

Abstract. Video measurements of swash were made at the low-sloping beach of the multiple bar system at Terschelling, Netherlands. The majority of the measurements were conducted under highly dissipative conditions with Iribarren numbers ξ_0 (the ratio of beach slope to the square root of offshore wave steepness) less than 0.2. Infragravity (0.004 - 0.05 Hz) waves dominated the swash with an average ratio of infragravity and total swash height R_{ig}/R of 0.85. Using linear regression we investigated the dependence of swash parameters on environmental conditions such as short-wave height, period, and local beach slope. On average, R_{ig} was about 30% of the offshore wave height H_0; the slope in the linear H_0 dependence of R_{ig} amounted to only 0.18, considerably smaller than that observed on steeper beaches. The data set shows evidence for saturation of the higher infragravity frequencies for ξ_0 less than, roughly, 0.27. In our opinion, this saturation caused the constant of proportionality in the linear relationship between R_{ig}/H_0 and ξ_0 to be significantly larger than that observed under higher Iribarren number regimes. The saturated tails of the swash spectra had an approximate f^{-3} roll-off (where f is frequency), whereas, in general, the nonsaturated parts were white. This lack of significant peaks casts doubt on the causality between infragravity waves and nearshore bars.

1. Introduction

Swash, the time-varying position of the shoreward edge of water on a beach, results from standing waves, formed by the reflection of incident waves off the shoreline [e.g., *Miche*, 1951; *Elgar and Guza*, 1985; *Guza and Thornton*, 1985; *Holland*, 1995]. There is still considerable debate as to how swash is related to environmental conditions such as local beach slope and offshore wave characteristics, despite the numerous studies that have been devoted to this subject.

Laboratory experiments with monochromatic waves on a plane beach have shown that vertical swash height R increases with growing incident wave height until R reaches a threshold value [*Miche*, 1951]. Any additional input of the incident wave energy is then dissipated in the surf zone and does not result in further growth of the vertical swash height, that is, the swash is saturated. It is unclear how *Miche*'s [1951] monochromatic swash results can be extended to random wave fields. *Huntley et al.* [1977] hypothesized that the saturated spectrum of vertical swash $R^2(f)$ of random waves is given by

$$R^2(f) = \epsilon^2 g^2 \beta^4 (2\pi f)^{-4} \quad (1)$$

where f is frequency, ϵ is a dimensional constant, g is the acceleration due to gravity, and β is the beach slope. Laboratory experiments with random waves, model predictions, and field observations have qualitatively confirmed Huntley et al.'s hypothesis [*Guza and Thornton*, 1982; *Mase and Iwagaki*, 1984; *Mizuguchi*, 1984; *Mase*, 1988; *Raubenheimer and Guza*, 1996]. They differ, however, in detail; in particular, the slope of the saturated region (on a log-log scale) varies between -3 and -4. *Guza and Thornton* [1982] speculated that these variations in the functional form of the spectral roll-off are related to differences in the applied measurement technique (video images or run-up wires; see also *Holman and Guza* [1984]), beach slope, and porosity. *Mase* [1988] observed f^{-4} spectral forms in the saturation region for (laboratory) beaches with slopes in the range from 1:5 to 1:30, thus suggesting that the f^{-3} and f^{-4} differences are independent of beach slope.

On natural beaches run-up at sea swell frequencies ($f >$ 0.05 Hz) is typically saturated (i.e., independent of the offshore wave height H_0), while swash at infragravity frequencies (0.004 - 0.05 Hz) is unsaturated and thus increases with H_0 [e.g., *Guza and Thornton*, 1982; *Holman and Sallenger*, 1985; *Holland*, 1995; *Holland et al.*, 1995]. There is, however, considerable debate as to how infragravity swash height R_{ig} and H_0 are related. For instance, *Guza and Thornton* [1982] and *Raubenheimer and Guza* [1996] observed a linear H_0 dependence of R_{ig}, with the constant of proportionality amounting to approximately 0.7. In contrast, *Holman and Sallenger* [1985] found the normalized infragravity swash height R_{ig}/H_0 to be linearly related to the Iribarren number ξ_0 as

$$\frac{R_{ig}}{H_0} = 0.53\xi_0 + 0.09 \quad (2)$$

where R_{ig} is the significant infragravity swash height, $\xi_0 = \tan\beta / \sqrt{(H_0/L_0)}$, and L_0 is the deep water wave length. They obtained (2) for ξ_0 varying between 0.5 and 3.5, approximating β by the local foreshore slope, H_0 by the offshore signi-

Paper number 97JC02791.
0148-0227/98/97JC-02791$09.00

ficant wave height defined as 4σ, where σ is the standard deviation of the sea surface elevation, and calculating L_0 with the peak period. Since the intercept in (2) is rather small, (2) suggests an approximate $H_0^{0.5}$ dependence of R_{ig}, in contrast to the aforementioned linear relationship. *Guza et al.* [1984] discussed the difference between findings of *Guza and Thornton* [1982] (who obtained their results under the range $0.3 < \xi_0 < 1.4$ based on their reported beach slopes, significant wave heights and peak frequencies) and *Holman and Sallenger* [1985] but were unable to resolve the discrepancy. *Holland* [1995] observed a relationship between R_{ig}/H_0 and ξ_0 for $0.4 < \xi_0 < 1.5$ similar to (2), although his intercept (0.34) was higher (*Holland* [1995] calculated R_{ig} and ξ_0 comparable to *Holman and Sallenger* [1985] but presented only alongshore-averaged values). *Holman and Bowen* [1984] reported a R_{ig}/H_0 value of 0.56 for a single measurement under dissipative conditions ($\xi_0 = 0.41$; the foreshore slope and their visually observed wave height and period were used to calculate ξ_0). It is unknown whether the observed relationships between R_{ig}, H_0, and ξ_0 are valid for situations outside the range of conditions under which they were obtained.

In this paper we present results from an extensive data set of swash obtained under highly dissipative conditions ($\xi_0 < 0.35$) on the beach of a multiple bar system. To the authors' knowledge, such conditions have not been presented in the literature so far. We address two issues: the dependence of the swash on environmental conditions and saturation. Similar to other observations on low-sloping beaches [e.g., *Guza and Thornton*, 1982; *Holland et al.*, 1995], we found that the swash mainly consisted of infragravity wave motions. In general, the saturation extended into the infragravity band, which had profound consequences for the relationship between the ratio R_{ig}/H_0 and ξ_0 compared to those existing for more reflective beach systems.

The outline of this paper is as follows. The applied methods are discussed in section 2. Results are presented in section 3, followed by a discussion in section 4, in which we compare our findings to previously observed dependencies of infragravity swash on environmental conditions. Finally, conclusions are summarized in section 5.

2. Methods

Swash data were collected at the low-sloping beach of the multiple bar system at Terschelling, Netherlands (Figure 1) during November 1993 and April and October 1994. The nearshore zone at the measurement site, which has an overall slope of about 0.005, is characterized by the presence of two or three bars that have a cross-shore spacing of several hundreds of meters [see also *Ruessink and Kroon*, 1994]. In the summer of 1993 a shoreface nourishment was executed by filling up the outer trough [*Hoekstra et al.*, 1994]. The intertidal zone, which has a slope of 0.01 to 0.03, frequently displays ridge-and-runnel features (Figure 2). The median grain size of the beach sand is 200 to 250 μm. The tide is semidiurnal with a neap and spring tidal range of about 1.2 and 2.5 m, respectively.

The swash was measured with video cameras that were mounted on the field research facility at the beach in section 17. The height of the cameras above mean sea level was about 9.5 m. Additional video recordings were obtained from a mobile platform. During each measurement, markers, which served as reference positions on the recordings, were placed on the beach in cross-shore transects. The alongshore spacing between the transects ranged from a few tens to several hundreds of meters depending on offshore wave conditions. The total data set consisted of 49 reliable runs. Forty-five of these runs were executed when the beach slope was less than 1:30, whereas the remaining four runs were performed on the steep seaward side of a swash bar with a slope of about 1:15. Measurements with intermediate (1:20 - 1:30) slopes were unavailable. The relationship between swash parameters and beach slope was found to be highly affected by the four slope outliers, an undesirable effect from a statistical point of view [e.g., *Blalock*, 1979]. As our main interest was focused primarily on the swash characteristics during highly dissipative conditions, we decided to select only the 45 runs with slopes less than 1:30 for further analysis and to discard the four outliers. The average number of cross-shore transects per measurement amounted to two or three. The swash recordings were mainly performed during high water

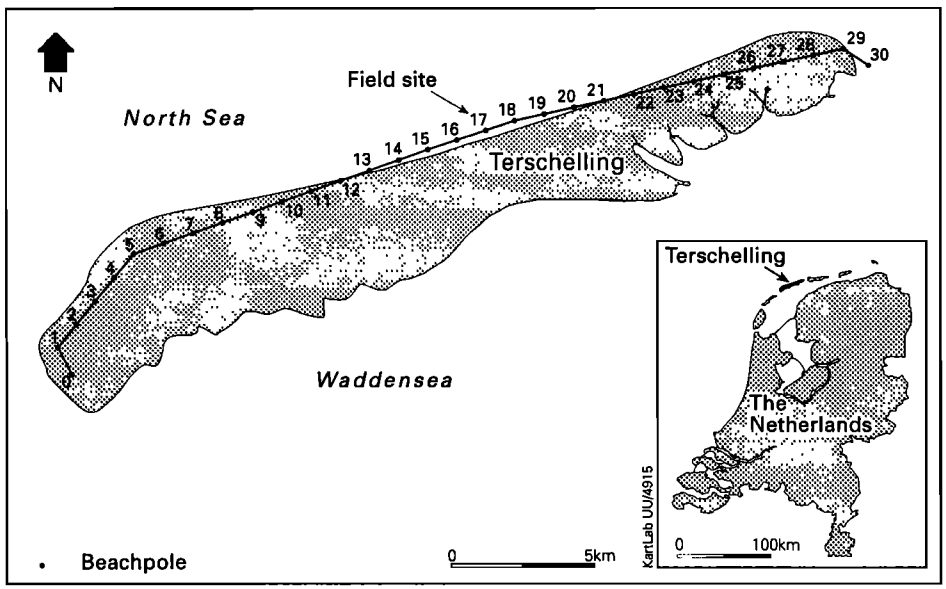

Figure 1. Measurement location.

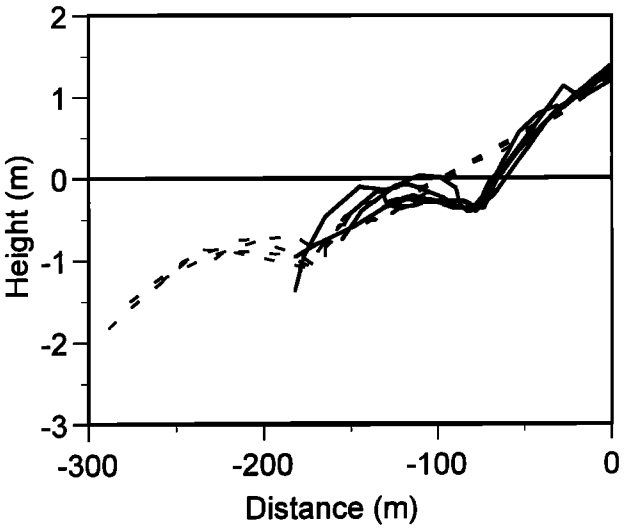

Figure 2. Selection of measured intertidal profiles. Solid lines, April 1994; dashed lines, October 1994. Distance is with respect to reference position on the beach; height is with respect to Dutch Ordnance Level (NAP). Mean water level is about 0 m NAP. Note that height is exaggerated enormously with respect to distance.

because the swash was almost invisible from the field research station during other stages of the tide.

The swash along the selected transects was manually digitized. As the height of the beach near the markers was accurately known, the beachface-parallel digitization resulted in time series of vertical swash elevation. The time series had a duration of about 45 min and a sampling frequency of 2 Hz. Energy spectra were computed from detrended, tapered, and 50% overlapping data segments of 1024 points (512 s), typically resulting in about 25 degrees of freedom. Swash heights were calculated as 4 times the square root of the zeroth-order spectral moment. The infragravity band was taken as 0.004 to 0.05 Hz, and the incident sea-swell band was taken as 0.05 to 0.33 Hz. Significant swash periods were calculated using a standard zero-down-crossing technique in the time domain.

Especially, the digitization of the backwash was prone to subjectivity between individual operators. The accuracy of the digitizations was analyzed by comparing the transect swash height, period, and spectral shape of the "individual" digitizations with the transect values averaged over the different operators. The individual values of height and period were generally within 5 to 10% of the mean value with the smaller deviations during more energetic offshore conditions. The spectral shape hardly varied between the different operators. In general, the differences between the swash statistics of the different transects of each measurement were insignificant; all swash parameters and spectra were therefore alongshore averaged.

Offshore wave conditions were measured by a directional wave buoy positioned 5 km offshore at a water depth of about 15 m. The (linear) bottom slope within the region of minimum run-down and maximum run-up of a recorded transect was taken as the beach slope. Both beach slope and Iribarren number (assuming $\tan\beta \approx \beta$) were alongshore averaged.

The left-hand part of Table 1 presents the measured offshore significant wave height, period T_0, steepness H_0/L_0 and angle of incidence α as well as the beach slope and Iribarren number of the present data set. The incident short waves were mainly sea dominated with swell being limited to only a few measurements (e.g., number 3). The offshore significant wave height and period were significantly linearly correlated at the 0.01 confidence level (correlation coefficient $r = 0.66$; correlations significantly different from 0 with 99% confidence have absolute values greater than 0.37). The offshore wave steepness generally increased during more energetic conditions (r between H_0 and H_0/L_0 amounted to 0.62). The variability in ξ_0 was about equally related to that in the square root of the offshore wave steepness ($r = -0.57$) and beach slope ($r = 0.47$).

3. Results

The observed significant swash height R, significant short-wave and infragravity swash height R_{ss} and R_{ig} as well as the significant swash period T_{sw} are shown in the right-hand part of Table 1. An overview of nondimensional swash parameters that can be deduced from Table 1 is given in Table 2. As can be seen in this table, the vertical swash was dominated by infragravity waves during most measurements with the ratio R_{ig}/R having a data set averaged value of 0.85. R_{ig} was about 30% of H_0. The significant swash period T_{sw} was, on average about 4 times as large as the incident short-wave period. The fluctuations in swash conditions experienced during our measurements were regressed against the environmental parameters listed in the left-hand part of Table 1. The correlation coefficients are shown in Table 3. It should be noted that the correlation coefficients between swash and offshore short-wave parameters must be interpreted with care, because some of the short-wave parameters were intercorrelated (see section 2). For this reason we will, if appropriate, also use the first-order partial correlation coefficients $r_{XY.Z}$ in the remainder of this paper, that is, the correlation between X and Y after Z has been allowed to explain all it can of both variables. Here X refers to a swash parameter, whereas Y and Z are intercorrelated environmental parameters.

As indicated by Table 3 and shown in Figure 3, the significant swash height R was significantly correlated to H_0. The slope of the best fit linear line was 0.18 and the intercept amounted to 0.24. Scatter around the general trend was related to variations in T_0 ($r_{R\text{T}0.H0} = 0.43$). In contrast to R, the largest part of the variability in T_{sw} was found to be related to T_0 (Figure 4). Part of the variance in T_{sw} unexplained by T_0 was related to H_0, such that the significant swash period grew with increasing offshore short-wave height ($r_{TswH0.T0} = 0.41$). In contrast to the findings of *Emery and Gale* [1951] and *McArdle and McLachlan* [1992], we observed no significant inverse relationship between T_{sw} and β, possibly related to the limited range of β values in our data set.

As can be seen in Figure 5, the growth of R with H_0 was mainly due to the increase in R_{ig}. The small constant of proportionality between R_{ss} and H_0 (0.04) and the strong β dependence of R_{ss} are qualitatively consistent with the saturation of short-wave swash. The dependence of R_{ss} on β was approximately equally well described by a linear (Table 3) and a quadratic fit (e.g., (1)). Variations in H_0/L_0 were found to be unrelated to the variance in R_{ss} unexplained by β and H_0. The best fit linear line relating R_{ig} and H_0 was given by

$$R_{ig} = 0.18H_0 + 0.17 \quad (3)$$

Table 1. Overview of Environmental Conditions and Dimensional Swash Parameters

Number	H_0, m	T_0, s	H_0/L_0	α*, deg	β	ξ_0	R, m	R_{ss}, m	R_{ig}, m	T_{sw}, s
					November 1993					
1	3.7	9.7	0.025	11	0.015	0.093	0.92	0.18	0.90	73.7
2	0.7	6.9	0.009	22	0.015	0.160	0.29	0.14	0.26	33.9
3	0.3	8.1	0.003	2	0.019	0.342	0.33	0.21	0.25	23.3
4	1.8	7.6	0.020	56	0.013	0.091	0.39	0.17	0.35	35.0
5	0.4	5.8	0.008	20	0.014	0.164	0.29	0.21	0.20	19.8
6	1.0	6.2	0.016	-54	0.012	0.098	0.28	0.15	0.25	33.4
7	1.1	6.4	0.017	-62	0.019	0.141	0.44	0.23	0.37	28.5
8	4.2	9.8	0.028	-56	0.013	0.078	0.68	0.27	0.63	48.2
9	4.5	10.2	0.028	-55	0.013	0.077	0.84	0.34	0.76	48.5
10	4.8	10.7	0.027	-54	0.019	0.115	1.19	0.40	1.11	54.8
11	3.1	8.7	0.026	-44	0.017	0.104	0.82	0.32	0.75	40.5
					April 1994					
12	1.3	6.5	0.019	32	0.030	0.218	0.60	0.43	0.41	19.5
13	2.8	7.7	0.030	6	0.032	0.187	0.81	0.54	0.61	19.9
14	3.7	10.3	0.022	7	0.015	0.104	0.95	0.36	0.88	48.1
15	3.8	10.8	0.021	6	0.013	0.092	0.96	0.35	0.89	54.6
16	3.4	10.0	0.022	8	0.015	0.099	0.89	0.30	0.84	60.5
17	3.4	10.6	0.019	2	0.016	0.119	0.77	0.27	0.72	53.0
18	2.2	8.9	0.018	20	0.016	0.124	0.69	0.30	0.62	40.8
19	2.4	8.4	0.021	20	0.020	0.135	0.72	0.32	0.65	39.1
20	2.4	8.4	0.022	22	0.021	0.145	0.90	0.38	0.81	39.6
21	2.2	8.8	0.019	14	0.018	0.132	0.64	0.27	0.57	34.3
22	2.0	7.8	0.021	12	0.013	0.088	0.40	0.19	0.35	35.9
23	1.8	7.5	0.021	11	0.020	0.138	0.64	0.33	0.55	34.7
24	1.8	7.5	0.020	10	0.025	0.177	0.68	0.44	0.53	20.6
25	1.4	5.1	0.033	17	0.019	0.104	0.41	0.27	0.31	23.8
26	1.4	5.1	0.035	16	0.019	0 100	0.45	0.32	0.32	20.1
27	1.6	5.6	0.033	15	0.019	0.103	0.50	0.33	0.38	21.1
28	1.7	5.5	0.035	11	0.023	0.125	0.59	0.42	0.41	22.1
29	0.6	5.6	0.013	-2	0.019	0.169	0.34	0.20	0.27	22.4
					October 1994					
30	2.8	9.0	0.022	1	0.018	0.120	0.94	0.35	0.87	47.5
31	1.1	8.3	0.010	-6	0.013	0.130	0.53	0.23	0.48	37.0
32	1.1	8.4	0.010	-9	0.016	0.153	0.53	0.26	0.46	33.7
33	1.1	10.4	0.006	7	0.013	0 164	0.60	0.20	0.56	46.0
34	1.0	9.9	0.007	9	0.014	0 172	0.52	0.20	0.48	45.2
35	1.8	8.2	0.017	13	0.009	0 068	0.51	0.20	0.47	52.1
36	0.9	10.0	0.006	10	0.017	0.222	0.59	0.26	0.53	38.3
37	0.8	9.8	0.006	11	0.010	0.134	0.52	0.22	0.47	40.0
38	0.5	5.0	0.012	-9	0.014	0.130	0.17	0.12	0.12	16.8
39	0.5	4.8	0.013	-5	0.014	0.125	0.19	0.14	0.12	16.4
40	0.5	5.0	0.012	-28	0.013	0.116	0.17	0.14	0.11	14.8
41	1.0	6.1	0.018	-61	0.011	0.085	0.25	0.14	0.21	26.1
42	3.8	9.7	0.026	-45	0.018	0.112	1.02	0.48	0.90	42.2
43	3.6	9.5	0.026	-41	0.016	0.102	0.89	0.31	0.83	52.7
44	1.3	8.2	0.012	-18	0.014	0.130	0.47	0.25	0.39	29.2
45	1.3	8.7	0.011	-14	0 011	0.108	0.41	0.23	0.34	30.0
Mean	2.0	8.0	0.019	-4	0.017	0.131	0.59	0.27	0.52	35.9
s.d.	1.2	1.8	0.008	28	0.005	0 048	0.25	0.10	0.25	13.6
Minimum	0.3	4.8	0.003	-62	0.009	0.068	0.17	0.12	0.11	14.8
Maximum	4.8	10.8	0.035	56	0.032	0 341	1 19	0.54	1.11	73.7

* Negative (positive) angle is west (east) of the shore normal direction.

The slope of this line is considerably smaller than the value of 0.7 observed by *Guza and Thornton* [1982]. In contrast to R_{ss}, R_{ig} proved to be sensitive to changes in T_0 ($r_{R_{ig}T0\,H0}$ = 0.60), suggesting that the input of infragravity energy into the swash zone grew with increasing offshore wave period. R_{ig} was found to be independent of β (Table 3).

In Figure 6 the ratio R_{ig}/H_0 is plotted against ξ_0. Note that the relationship between ξ_0 and R_{ig}/H_0 was entirely due to

Table 2. Overview of Nondimensional Swash Parameters

	R_{ss}/R	R_{ig}/R	R/H_0	R_{ss}/H_0	R_{ig}/H_0	T_{sw}/T_0
Mean	0.50	0.85	0.37	0.19	0.31	4.38
s.d.	0.14	0.09	0.16	0.12	0.13	0.97
Minimum	0.19	0.63	0.16	0.05	0.15	2.58
Maximum	0.78	0.98	1.02	0.65	0.79	7.60

dependence of R_{ig}/H_0 on the offshore wave steepness (Table 3). The best fit linear line relating R_{ig}/H_0 and ξ_0 was

$$\frac{R_{ig}}{H_0} = 2.20\xi_0 + 0.02 \quad (4)$$

The slope in (4) is significantly larger than the one in (2). Since the intercept in (4) is small, the linear relationship between R_{ig}/H_0 and ξ_0 suggests an approximate $H_0^{0.5}$ dependence of the unnormalized infragravity swash (R_{ig}), which is in contrast with the linear relationship given in Figure 5. The correlation coefficient between R_{ig} and $H_0^{0.5}$ amounted to 0.89, which is equal to the one for the linear H_0 dependence of R_{ig}. Therefore we cannot distinguish statistically between a linear and a nonlinear relationship between the significant infragravity swash height and the offshore short-wave height.

Figure 7 shows a representative selection of swash energy spectra of the present data set. As can be seen in this figure, the largest variability in swash energy occurred at infragravity frequencies (note that the standard deviation of R_{ig} computed from the entire data set was 2½ times as large as that of R_{ss} (Table 1)). The saturated tails decayed approximately as f^{-3}. The unsaturated parts were generally white, in other words, lacked significant peaks; such peaks were detected during only 4 of the 45 measurements. For all 45 alongshore-averaged spectra we determined the approximate position of the knickpoint between the saturated and unsaturated part as follows. First, a best fit line of the form f^{-b} (where $-b$ is the slope on a log-log scale) was obtained through the energy in the frequency range 0.1 - 0.33 Hz. Second, this line was extrapolated to lower frequencies, and finally, the knickpoint was taken as the lowest frequency still having energy not significantly different from this extrapolated line. Hereinafter, this frequency is referred to as the lowest saturated frequency f_s. As shown in Figure 7, f_s was generally less than 0.05 Hz; that is, the saturated tail extended into the infragravity-frequency band.

We subsequently divided the infragravity-frequency band into three classes, namely, $0.004 \le f \le 0.018$ Hz, $0.018 < f \le 0.033$ Hz, and $0.033 < f \le 0.05$ Hz, and determined the swash height for each class. The result is shown in Figure 8. The heights of the three frequency bands were about the same for H_0 less than 1 m, caused by the white infragravity spectra under these conditions. Only the height of the lowest frequency band increased approximately linearly with H_0 during more energetic conditions, whereas the growth in the height of the highest frequency band and the midfrequency band were arrested (i.e., full saturation) at a value of $H_0 \approx 2$ m and $H_0 \approx 3$ m, respectively. Clearly, f_s shifted to lower infragravity frequencies under more energetic conditions (r between f_s and H_0 amounted to -0.50).

Figure 9 shows the lowest saturated frequency plotted against ξ_0 ($r = 0.43$). Note that omitting the extreme value of $\xi_0 = 0.35$ from the regression analysis still resulted in a significant ξ_0 dependence of f_s. The linear solution from the regression analysis shows that for $\xi_0 < 0.27$ f_s was within the infragravity-frequency range, although errors in this value may be considerable given the weakness of the relationship. Nonetheless, we think that the downshift in f_s inside the infragravity band caused the slope in the ξ_0 dependence of R_{ig}/H_0 (equation (4); Figure 6) to be profoundly steeper than those observed at more reflective beach systems. Because of the growth in saturated energy levels with decreasing frequency (equation (1); Figure 7), the nondimensional swash period (T_{sw}/T_0) increased under more dissipative conditions (Table 3).

4. Discussion

In a recent review paper on the hydrodynamics of infragravity waves, *Huntley et al.* [1993] argued that the $0.7H_0$ dependence of R_{ig} based on *Guza and Thornton*'s [1982] data was the best choice for modeling infragravity swash wave amplitude on dissipative beaches (the Iribarren number in Guza and Thornton's experiments varied between 0.3 and 1.4; see section 1). Under even more dissipative conditions, however, we observed a data set averaged value of R_{ig}/H_0 of 0.30 (Table 3) and a constant of proportionality in the linear H_0 dependence of R_{ig} of only 0.18 (Figure 5). This suggests that in some way the ratio R_{ig}/H_0 depends on the Iribarren number [see also *Howd et al.*, 1991].

Table 3. Correlation Coefficients Between Environmental and Swash Parameters

	R	R_{ss}	R_{ig}	T_{sw}	R_{ss}/R	R_{ig}/R	R/H_0	R_{ss}/H_0	R_{ig}/H_0	T_{sw}/T_0
H_0	0.88	0.56	0.89	0.72	-0.62	0.58	-0.65	-0.71	-0.55	0.53
T_0	0.74	(0.27)	0.80	0.84	-0.85	0.84	(-0.14)	-0.47	(0.07)	0.44
H_0/L_0	0.48	0.60	0.41	(0.12)	(-0.01)	(-0.02)	-0.70	-0.51	-0.74	(0.25)
α	(-0.10)	(0.04)	(-0.13)	(-0.11)	(0.10)	(-0.12)	(0.24)	(0.21)	(0.23)	(-0.09)
β	(0.27)	0.73	(0.14)	(-0.34)	(0.36)	(-0.35)	(0.07)	(0.21)	(-0.02)	-0.40
ξ_0	(-0.19)	(0.07)	(-0.23)	(-0.37)	(0.31)	(-0.28)	0.85	0.78	0.80	-0.55

Correlation coefficients insignificant at 0.01 confidence level have absolute values less than 0.38 and are shown in parentheses. All correlation coefficients between swash parameters and the angle of incidence are insignificant and are therefore not discussed in the text.

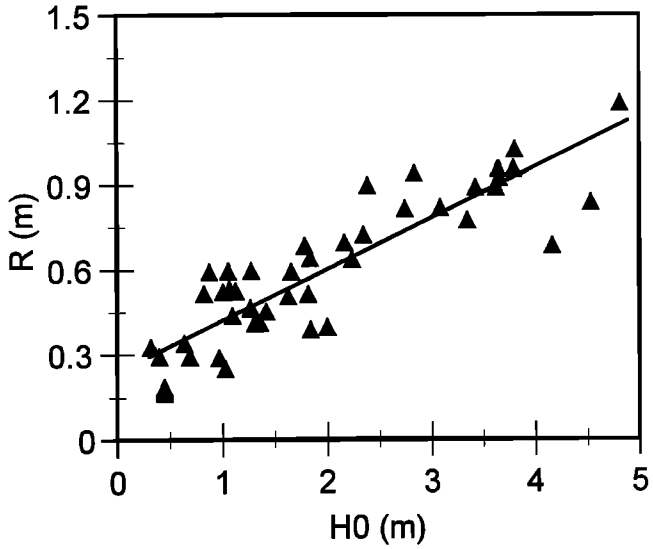

Figure 3. Observed swash height R versus offshore wave height H_0. The solid line is the best fit linear line: $R = 0.18H_0 + 0.24$ ($r = 0.88$).

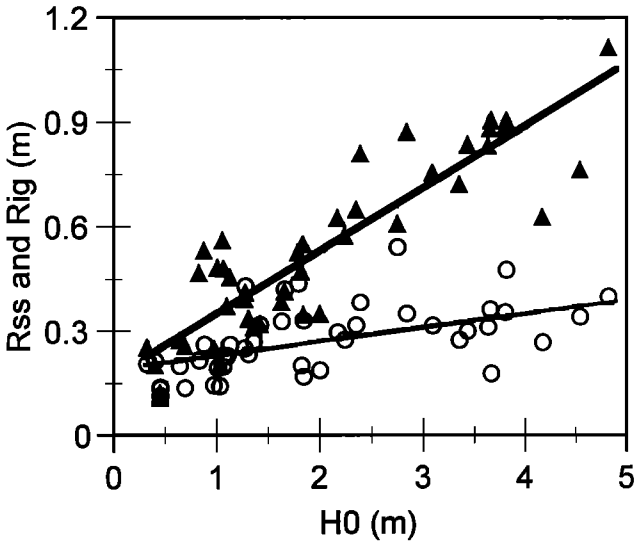

Figure 5. Observed infragravity swash height R_{ig} (solid triangles) and sea swell swash height R_{ss} (open circles) versus offshore wave height H_0. The thick line is $R_{ig} = 0.18H_0 + 0.16$ ($r = 0.89$); the thin line is $R_{ss} = 0.04H_0 + 0.19$ ($r = 0.56$).

Figure 10 presents an overview of the measured ξ_0 dependencies of R_{ig}/H_0 published in the literature together with our findings. Clearly, the slope in the ξ_0 relationship we observed is significantly larger than the ones measured on more reflective beaches. We ascribe this difference to the saturation of the higher infragravity frequencies for situations with ξ_0 less than, roughly, 0.27 (Figure 9). Interestingly, *Raubenheimer and Guza*'s [1996] data showed a slight decrease in the ratio R_{ig}/H_0 for their most dissipative conditions ($\xi_0 \approx 0.3$ - 0.6). Whether this decrease can actually be seen as a transition toward the ξ_0 dependence we measured cannot be established unambiguously because of the lack of sufficient data points in the ξ_0 range from 0.2 to 0.6. Note that *Raubenheimer and Guza*'s [1996] and our observations can be approximated by $R_{ig}/H_0 = 0.65 \tanh(3.38\xi_0)$. For highly dissipative conditions this equation reduces to (4), whereas for more reflective conditions it loses its ξ_0 dependence and attains a constant value of 0.65.

Remarkably, different relationships between ξ_0 and R_{ig}/H_0 seem to exist for $\xi_0 > 0.3$. In *Holman and Sallenger*'s [1985] and *Holland*'s [1995] data set (lines b and c, respectively) the variability in ξ_0 was mainly determined by the wave steepness. On the other hand, in the data of *Raubenheimer and Guza* [1996] (line d) the range of beach slopes was much greater than the range of wave steepness. Instrumental differences and different calculations methods of R_{ig} (e.g., alongshore averaging [*Holland*, 1995] or not [*Holman and Sallenger*, 1985]) may explain the various dependencies partly. Re-

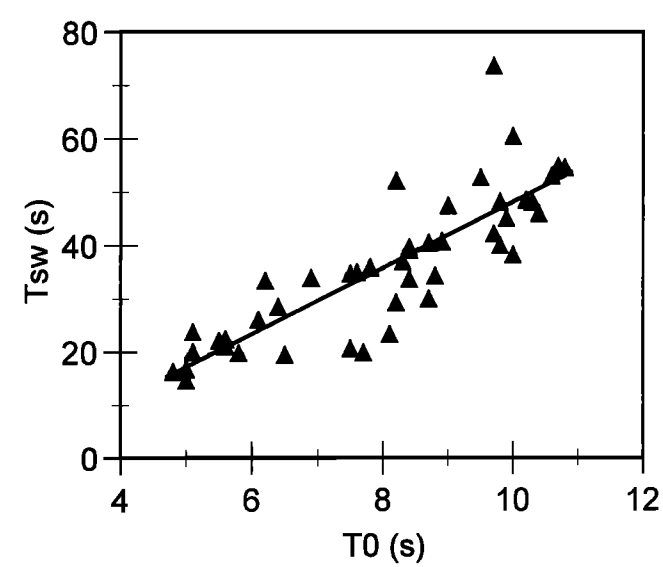

Figure 4. Observed significant swash period T_{sw} versus offshore wave period T_0. The solid line is the best fit linear line: $T_{sw} = -13.67 + 6.18T_0$ ($r = 0.84$).

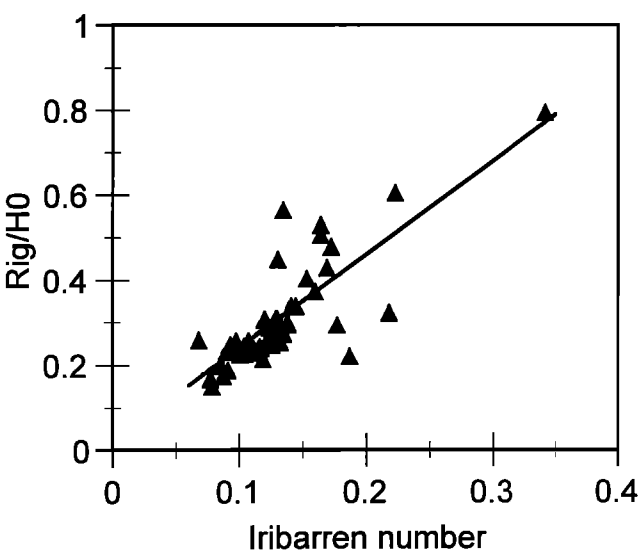

Figure 6. Observed ratio between infragravity swash height and offshore wave height R_{ig}/H_0 versus Iribarren number ξ_0. The solid line represents the best fit linear line: $R_{ig}/H_0 = 2.20\xi_0 + 0.02$ ($r = 0.80$).

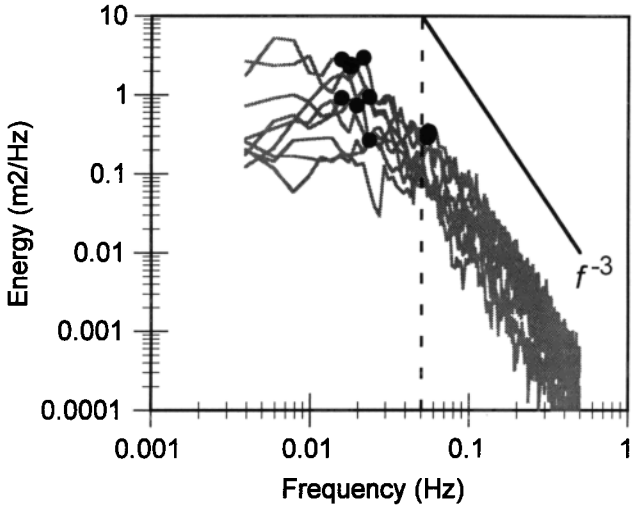

Figure 7. Selection of vertical swash spectra of the present data set. The vertical dashed line is the division between the infragravity and sea swell band (f = 0.05 Hz). The black line shows the f^{-3} dependence of swash energy. The solid circles denote the transition between the saturated tails and the nonsaturated parts (see text for explanation).

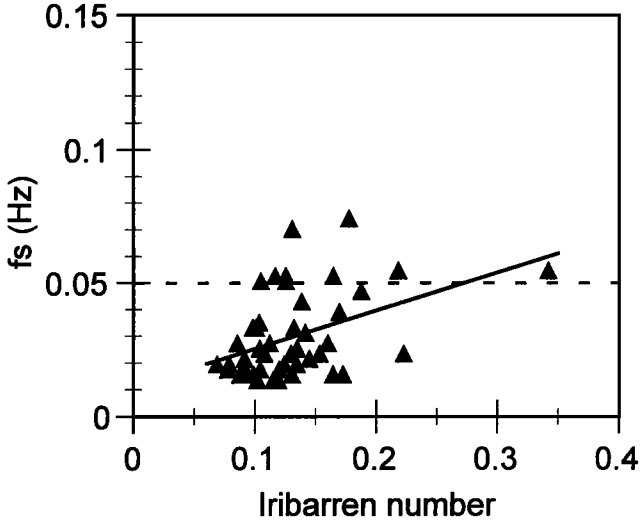

Figure 9. Lowest saturated frequency f_s versus Iribarren number ξ_0. The horizontal dashed line is the division between the infragravity and sea swell band (f = 0.05 Hz). The solid line is the best linear fit: $f_s = 0.143\ \xi_0 + 0.011$ (r = 0.43).

cently, *Raubenheimer and Guza* [1996] doubted whether a generally valid dependence of R_{ig}/H_0 on ξ_0 may exist at all, that is, whether an observed relationship may not be site specific. Observations in intermediate water depths (10 - 30 m) have revealed that the amount of infragravity energy does not only depend on local short-wave parameters but may also be a function of the large-scale morphology like shelf width [*Herbers et al.*, 1995]. Herbers et al. observed markedly different amounts of infragravity energy at the same depths on shelves with various widths, presumably related to the different degrees of trapping of the free infragravity motions present. Clearly, these differences are not accounted for by a local parameter such as the Iribarren number.

Our field observations cast doubt on the causality between infragravity waves and nearshore bars. The nonsaturated part of the vertical swash spectra lacked significant peaks, which would be present in case of resonance over the barred morphology [*Kirby et al.*, 1981; *Symonds and Bowen*, 1984]. Similar observations on barred beaches have been reported in, for instance, *Holman and Sallenger* [1993] and *Holland* [1995]. A standing infragravity wave field having a white shoreline spectrum does not result in a net sediment transport [e.g., *Holman and Sallenger*, 1993; *Aagaard and Greenwood*, 1994] and, accordingly, cannot form or modify nearshore bars. In addition, the saturation of the higher infragravity frequencies implies that the reflection coefficient at

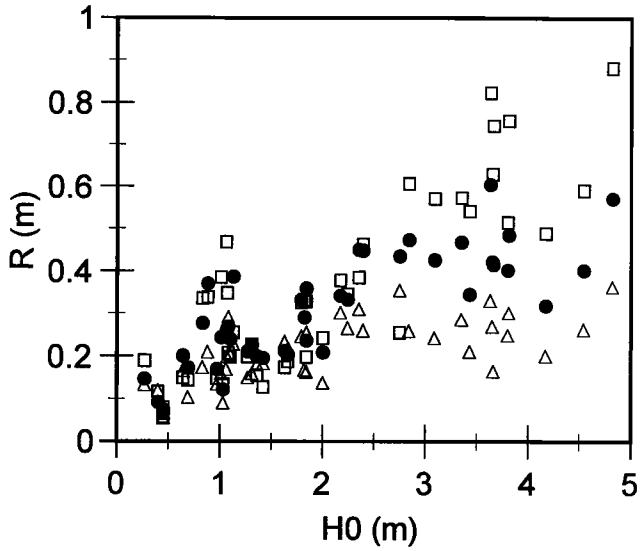

Figure 8. Observed swash height R for frequency bands $0.004 \le f \le 0.018$ Hz (open squares), $0.018 < f \le 0.033$ Hz (solid circles) and $0.033 < f \le 0.05$ Hz (open triangles) versus offshore wave height H_0.

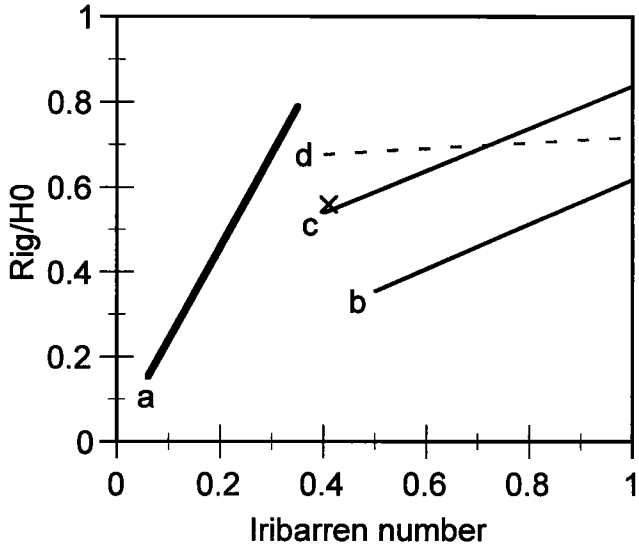

Figure 10. Overview of published ξ_0 dependencies of R_{ig}/H_0. Line a represents (4): $R_{ig}/H_0 = 2.20\ \xi_0 + 0.02$. The sloping line b is $R_{ig}/H_0 = 0.53\ \xi_0 + 0.09$ [*Holman and Sallenger*, 1985], line c is $R_{ig}/H_0 = 0.50\ \xi_0 + 0.34$ [*Holland*, 1995], and the dashed line d is $R_{ig}/H_0 = 0.07\ \xi_0 + 0.65$ [*Raubenheimer and Guza*, 1996]. The single cross represents *Holman and Bowen*'s [1984] data.

these frequencies is less than unity, whereas most models that relate nearshore bars and infragravity waves rely on a full-standing wave field. More work on the generation and modification of nearshore bars is clearly needed.

5. Conclusions

Infragravity wave motions (0.004 - 0.05 Hz) dominate the swash on the gently sloping beach (on average 1:60) of the present field site. The data set averaged contribution of infragravity waves, expressed as the ratio R_{ig}/R, is about 0.85. The constant of proportionality in the linear H_0 dependence of R_{ig} amounts to only 0.18, which is considerably smaller than the value of 0.7 observed by *Guza and Thornton* [1982] on a steeper beach. In contrast to more reflective beach systems, the high-frequency part of the infragravity waves is saturated for ξ_0 less than, roughly, 0.27. Because of the decrease in f_s inside the infragravity band under more dissipative conditions (Figure 9), the slope in the linear ξ_0 dependence of R_{ig}/H_0 we observed is considerably steeper than that for higher Iribarren regimes reported in the literature. The functional form of the saturated parts of the swash energy spectra is a f^{-3} roll-off, whereas the unsaturated parts are generally constant with frequency. This lack of significant spectral peaks casts doubt on the causality between infragravity waves and (multiple) bars.

Acknowledgments. Part of this work was supported by the NOURTEC project: Innovative Nourishment Techniques, which was jointly funded by the Ministry of Transport, Public Works and Water Management in the Netherlands and by the Commission of the European Communities, Directorate General for Science, Research and Development under the Marine Science and Technology programme contract MAS2-CT93-0049. The paper was greatly improved by incorporating the valuable comments from two reviewers.

References

Aagaard, T., and B. Greenwood, Suspended sediment transport and the role of infragravity waves in a barred surf zone, *Mar. Geol.*, *118*, 23-48, 1994.

Blalock, H.M. Jr., *Social Statistics*, 2nd ed., 625 pp., McGraw-Hill, New York, 1979.

Elgar, S., and R.T. Guza, Observations of bispectra of shoaling surface gravity waves, *J. Fluid Mech.*, *161*, 425-448, 1985.

Emery, K.O., and J.F. Gale, Swash and swash marks, *Trans. AGU*, *32*, 31-36, 1951.

Guza, R.T., and E.B. Thornton, Swash oscillations on a natural beach, *J. Geophys. Res.*, *87*, 483-491, 1982.

Guza, R.T., and E.B. Thornton, Observations of surf beat, *J. Geophys. Res.*, *90*, 3161-3172, 1985.

Guza, R.T., E.B. Thornton, and R.A. Holman, Swash on steep and shallow beaches, in *Proceedings of the 19th International Conference on Coastal Engineering*, pp. 708-723, Am. Soc. of Civ. Eng., Reston, Va., 1984.

Herbers, T.H.C., S. Elgar, R.T. Guza, and W.C. O'Reilly, Infragravity-frequency (0.005-0.05 Hz) motions on the shelf, II, Free waves, *J. Phys. Oceanogr.*, *25*, 1063-1079, 1995.

Hoekstra, P., K.T. Houwman, A. Kroon, P. van Vessem, and B.G. Ruessink, The Nourtec experiment of Terschelling: Process-oriented monitoring of a shoreface nourishment (1993-1996), in *Proceedings of Coastal Dynamics '94*, pp. 402-416, Am. Soc. of Civ. Eng., Reston, Va., 1994.

Holland, K.T., Foreshore dynamics: Swash motions and topographic interactions on natural beaches, Ph.D. thesis, 119 pp., Oreg. State Univ., Corvallis, 1995.

Holland, K.T., B. Raubenheimer, R.T. Guza, and R.A. Holman, Runup kinematics on a natural beach, *J. Geophys. Res.*, *100*, 4985-4993, 1995.

Holman, R.A., and A.J. Bowen, Longshore structure of infragravity wave motions, *J. Geophys. Res.*, *89*, 6446-6452, 1984.

Holman, R.A., and R.T. Guza, Measuring run-up on a natural beach, *Coastal Eng.*, *8*, 129-140, 1984.

Holman, R.A., and A.H. Sallenger, Setup and swash on a natural beach, *J. Geophys. Res.*, *90*, 945-953, 1985.

Holman, R.A., and A.H. Sallenger, Sand bar generation: A discussion of the Duck experiment series, *J. Coastal Res.*, special issue, *15*, 76-92, 1993.

Howd, P.A., J. Oltman-Shay, and R.A. Holman, Wave variance partitioning in the trough of a barred beach, *J. Geophys. Res.*, *96*, 12781-12795, 1991.

Huntley, D.A., R.T. Guza, and A.J. Bowen, A universal form for shoreline run-up spectra?, *J. Geophys. Res.*, *82*, 2577-2581, 1977.

Huntley, D.A., M. Davidson, P. Russell, Y. Foote, and J. Hardisty, Long waves and sediment movement on beaches: Recent observations and implications for modelling, *J. Coastal Res.*, special issue, *15*, 215-229, 1993.

Kirby, J.T., Jr., R.A. Dalrymple, and P. L.-F. Liu, Modification of edge waves by barred-beach topography, *Coastal Eng.*, *5*, 35-49, 1981.

Mase, H., Spectral characteristics of random wave run-up, *Coastal Eng.*, *12*, 175-189, 1988.

Mase, H., and Y. Iwagaki, Run-up of random waves on gentle slopes, in *Proceedings of the 19th International Conference on Coastal Engineering*, pp. 593-609, Am. Soc. of Civ. Eng., Reston, Va., 1984.

McArdle, S.B., and A. McLachlan, Sand beach ecology: Swash features relevant to the macrofauna, *J. Coastal Res.*, *8*(2), 398-407, 1992.

Miche, R., Le pouvoir réfléchissant des ouvrages maritimes exposés à l'action de la houle, *Ann. Ponts Chaussees*, *121*, 285-319, 1951.

Mizuguchi, M., Swash on a natural beach, in *Proceedings of the 19th International Conference on Coastal Engineering*, pp. 678-694, Am. Soc. of Civ. Eng., Raston, Va.,1984.

Raubenheimer, B., and R.T. Guza, Observations and predictions of run-up, *J. Geophys. Res.*, *101*, 25575-25587, 1996.

Ruessink, B.G., and A. Kroon, The behaviour of a multiple bar system in the nearshore zone of Terschelling, the Netherlands: 1965-1993, *Mar. Geol.*, *121*, 187-197, 1994.

Symonds, G., and A.J. Bowen, Interactions of nearshore bars with incoming wave groups, *J. Geophys. Res.*, *89*, 1953-1959, 1984.

M. G. Kleinhans, B.G. Ruessink, and P. G. L. van den Beukel, Institute for Marine and Atmospheric Research Utrecht, Department of Physical Geography, Utrecht University, P.O. Box 80.115, 3508 TC Utrecht, Netherlands. (e-mail: m.kleinhans@frw.ruu.nl; b.ruessink@frw.ruu.nl)

(Received May 31, 1996; revised June 30, 1997;
accepted August 8, 1997.)